Effect of Modification of Oxide Layer on NiTi Stent Corrosion Resistance

Trepanier, Tabrizian, Yahia, Bilodeau, Piron

1997

Effect of Modification of Oxide Layer on NiTi Stent Corrosion Resistance

Christine Trépanier,[1] Maryam Tabrizian,[1] L'Hocine Yahia,[1] Luc Bilodeau,[2] Dominique L. Piron[3]

[1] GRBB, Biomedical Engineering Institute, École Polytechnique de Montréal, Montreal, Quebec H3C 3A7, Canada

[2] Institut de Cardiologie de Montréal, Montreal, Quebec H3C 3A7, Canada

[3] Department of Material Engineering, École Polytechnique de Montréal, Montreal, Quebec H3C 3A7, Canada

Received 22 July 1997; accepted 8 December 1997

Abstract: Because of its good radiopacity, superelasticity, and shape memory properties, nickel-titanium (NiTi) is a potential material for fabrication of stents because these properties can facilitate their implantation and precise positioning. However, *in vitro* studies of NiTi alloys report the dependence of alloy biocompatibility and corrosion behavior on surface conditions. Surface oxidation seems to be very promising for improving the corrosion resistance and biocompatibility of NiTi. In this work, we studied the effect on corrosion resistance and surface characteristics of electropolishing, heat treatment, and nitric acid passivation of NiTi stents. Characterization techniques such as potentiodynamic polarization tests, scanning electron microscopy, Auger electron spectroscopy, and X-ray photoelectron spectroscopy were used to relate corrosion behavior to surface characteristics and surface treatments. Results show that all of these surface treatments improve the corrosion resistance of the alloy. This improvement is attributed to the plastically deformed native oxide layer removal and replacement by a newly grown, more uniform one. The uniformity of the oxide layer, rather than its thickness and composition, seems to be the predominant factor to explain the corrosion resistance improvement. © 1998 John Wiley & Sons, Inc. J Biomed Mater Res (Appl Biomater) 43: 433–440, 1998

Keywords: NiTi shape memory alloy; stents; surface treatments; corrosion resistance; surface characterization

INTRODUCTION

Since 1986, implantation of tubular endoprostheses (stents) in blood vessels has been performed in humans to prevent occlusion and restenosis of coronary arteries after a percutaneous intervention like angioplasty.[1] These devices constitute one of the most effective ways to treat coronary stenosis. Clinical results have demonstrated a decrease of at least 30% of the restenosis rate after their implantation.[2,3] However, clinically used stainless steel- and tantalum-based metallic stents have limitations because of their suboptimal radiopacity and mechanical properties that may complicate the insertion and positioning of stents at the site of obstruction.[4] In contrast, optimal radiopacity, superelasticity, and shape memory properties make nickel-titanium (NiTi) an attractive material for such an application. Indeed, these properties can facilitate the positioning of the stents for a precise implantation. However, before any new alloy can be approved for implantation in the human body, the biocompatibility of the material must be established. Berger–Gorbet et al.'s recent study underlined the slower osteogenesis process associated with NiTi by *in vivo* implantation of nontreated NiTi screws in the tibias of rabbits.[5] This finding was associated with the release of a cytotoxic constituent by NiTi during corrosion of the alloy. Among the factors that determine the biocompatibility of an implant, surface properties and corrosion resistance are the most important characteristics of the material. *In vitro* studies of NiTi in contact with different cell cultures demonstrated the dependence of the alloy biocompatibility behavior on surface treatments.[6–8] Indeed, passive metals like NiTi have a stable oxide layer on their surface that helps to render them corrosion resistant and relatively inert in physiological conditions. This passivity may be enhanced by modifying the thickness, topography, and chemical composition of this oxide layer by different surface treat-

Correspondence to: Dr. M. Tabrizian (e-mail: tabrizia@grbb.polymtl.ca)
Contract grant sponsor: NSERC (Canada)
Contract grant sponsor: Nitinol Devices & Components Inc. (California)

 CCC 0021-9304/98/040433-08

ments.[7,9,10] This improved oxide layer has been shown to be very protective and promising for improving the corrosion resistance and biocompatibility of NiTi.[9-11] Also, Sohmura showed that this layer is able to sustain large deformations induced by the shape memory effect.[10]

Several surface treatments have been developed such as the laser surface melting technique, which promotes the oxidation of NiTi and improves the corrosion resistance of the alloy.[9] However, this technique is expensive and inappropriate for implants like stents due to their complex geometry. Modification of the oxide layer can also be achieved by more conventional methods such as chemical polishing and heat treatment.[12] A study of Ti-based implants demonstrated a reduction of ion dissolution by aging of the surface oxide or by thermal oxidation.[13] Electropolishing and nitric acid passivation are two other techniques recommended for surface treatment of medical devices to remove deformed native oxide layers and replace them by more uniform ones (ASTM-F86).[14] These methods are simple, inexpensive, and effective in treating implants of different shapes and geometries.

The primary goal of this study was to investigate the effect of electropolishing, heat treatment (in air and in a salt bath), and nitric acid passivation on the corrosion behavior of NiTi stents by potentiodynamic anodic polarization tests. The second objective was to describe the relationships between corrosion behavior, surface characteristics, and surface treatment of NiTi stents by using scanning electron microscopy (SEM) to study the topography and Auger electron spectroscopy (AES) and X-ray photoelectron spectroscopy (XPS) to analyze the chemical composition of the oxide layer.

MATERIALS AND METHODS

The NiTi stents (50.8 atom % Ni) were manufactured by Nitinol Devices & Components and consisted of rigid slotted tubes 4 mm in diameter (expanded state) and 14 mm in length where laser-cut rows of rectangles became diamond-shaped apertures in the expanded state. Five different groups of samples were prepared: nontreated (NT), electropolished (EP), air aged (AA), heat treated (HT), and passivated (PA). The control group of stents (NT) were supplied with a self-generated heavy oxide layer formed directly after the machining and expansion. EP stents were first microabraded to remove the primary oxide layer mechanically, then chemically polished at room temperature, and finally electropolished according to standard electropolishing techniques for NiTi to obtain a mirrorlike surface finish. AA samples were EP stents that had been aged at 450 °C for a few minutes, resulting in a surface covered with a light yellow oxide layer. The HT stents were EP stents heated in a standard nitrite/nitrate salt bath at 500 °C for a few minutes until obtention of a dark blue oxide layer. The chemically PA stents were EP stents that had been passivated in a 10% nitric acid solution at room temperature according to the ASTM-F86 standard.[14] They exhibited the same optical surface finish as the EP stents. All surface treatments described in this article were performed by Nitinol Devices & Components.

The corrosion resistance of the stents was evaluated by anodic polarization tests. The potentiodynamic experiments were carried out using a computer-controlled potentiostat (EG&G Princeton Applied Research, model 273). The tests were conducted in 37 °C Hank's physiological solution with the following composition: NaCl, 8 g/L; KCl, 0.4 g/L; $NaHCO_3$, 0.35 g/L; KH_2PO_4, 0.06 g/L; Na_2HPO_4, 0.0475 g/L; and $C_6H_{12}O_6$ (glucose), 1 g/L. This solution was buffered with HEPES (3.5745 g/L) at the normal physiological pH of 7.4. A saturated calomel electrode (SCE) was used as the reference and platinum as the counter electrode. The solution was deoxygenated with nitrogen gas for 1 h before starting the experiment. The samples were immersed 30 min prior to the test to stabilize the open circuit potential (OCP). A scan rate of 10 mV/min was applied starting from the OCP until obtention of the sample pitting potential. For reproducibility of results, all corrosion tests were performed continuously over a short period of time.

SEM

A Jeol JSM 840 microscope was used to study the topography of samples before and after corrosion tests. Micrographs were taken at areas located on the external and lateral faces of the stents in the second electron imaging mode.

AES

The AES analyses were performed on samples before and after corrosion experiments with a Jeol JAMP 30 microscope. AES survey spectra (100–1200 eV) were recorded from two different spots (5 μm^2) on the external faces of each sample to identify the surface composition. Then depth profiles were measured by combining AES analysis and argon ion sputter etching to evaluate the oxide layer thickness and the distribution of each element in the sample. Oxide thickness was evaluated from the sputtering time required to decrease the O signal in the oxide halfway from its initial intensity to the background noise level. The thickness in terms of sputtering time was converted to angstroms by using the sputtering rate of an SiO_2 standard (100 Å/min), assuming that the sputtering rate was equivalent for NiTi oxide.

XPS

The XPS measurements were performed with a vacuum generator ESCALAB 3 MK II spectrometer, using Al Kα radiation on samples before and after the corrosion experi-

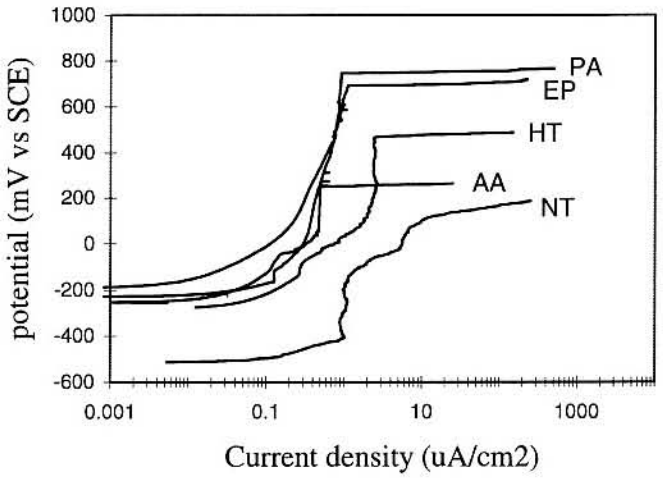

Figure 1. Typical potentiodynamic scanning curves.

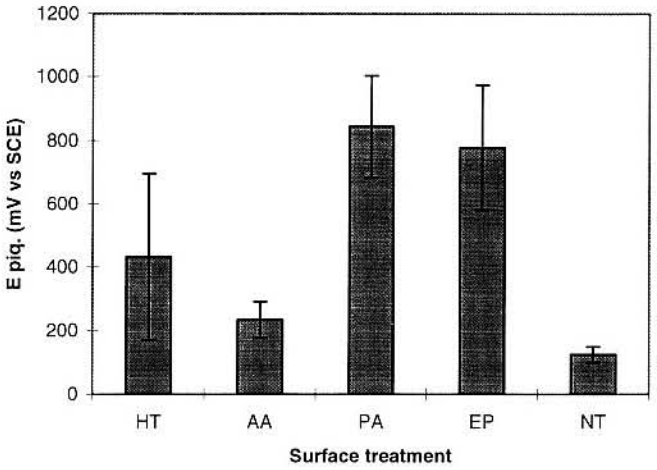

Figure 2. Variation of pitting potential as a function of surface treatment.

ments. To remove salts from the physiological solution, all corroded stents were cleaned with deionized water in an ultrasound bath for 5 min prior to the analyses. An angulation of 20 ° of the specimens was used to maximize the signal from the surface of the NiTi sample. The data were collected and analyzed by a PC-AT computer. Atomic percentages of titanium and nickel were derived by survey spectra. The sensitivity factors used were 1.8 for Ti and 4.5 for Ni.[15] Furthermore, high resolution XPS spectra of C 1*s*, O 1*s*, Ni 2*p*, and Ti 2*p* regions were also performed to determine the nature of their chemical bonds. Binding energies and peak areas were determined by using curve-fitting routines provided by a Sursoft program. Due to the special shape of the stents, a copper sample holder was used for easy identification of any peak contribution from this device on the survey scans.

RESULTS

Typical potentiodynamic scanning curves for each surface condition are illustrated in Figure 1. These scanning curves reveal an increase of the pitting potential of treated samples ranging from 100 to 600 mV and a decrease of their passivation current density when compared to the control group (NT). Figure 2 shows the variation of the pitting potential with regard to surface treatments.

Before the corrosion experiment, NT stents exhibited a very porous and irregular surface topography (Fig. 3). After all treatments, the stent surface appeared smoother and more uniform (Fig. 4, EP stent). However, some surface cracks were visible on the lateral faces of devices at the end point of the diamond apertures (Fig. 5).

Machining scratches were also apparent on the external faces of all samples. Still, the topography was not uniform on all faces of the devices for different surface treatments. Indeed, the oxide layer on the lateral faces of the HT and AA treated stents seemed irregular compared to the external faces.

After the corrosion experiment, SEM analyses revealed that the corrosion process was more severe on lateral surfaces of all devices. Figures 6 and 7 compare the local corrosion process of the external and lateral faces of the AA stent.

Before and after the corrosion experiment the AES survey spectra demonstrated the presence of C, Ti, and O on all the devices. Except on the AA stents, small signals from Ni could also be randomly recorded on the survey scans. Signals from Ca, P, S, and Cl were also randomly observed; these were attributed to the contamination of samples during manipulations and/or to the physiological solution used for the corrosion tests. No significant differences between AES survey scans and depth profiles were observed among the corroded and noncorroded specimens.

AES depth profiles of O, Ti, and Ni from the surface

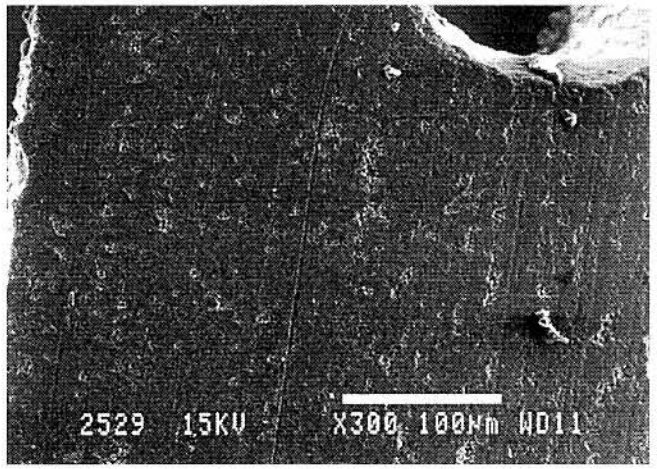

Figure 3. Porous and irregular surface of nontreated stent.

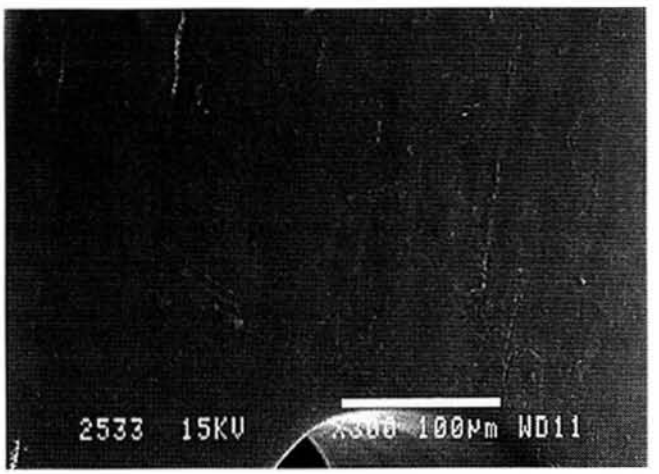

Figure 4. Typical smooth and uniform topography of treated stent (EP).

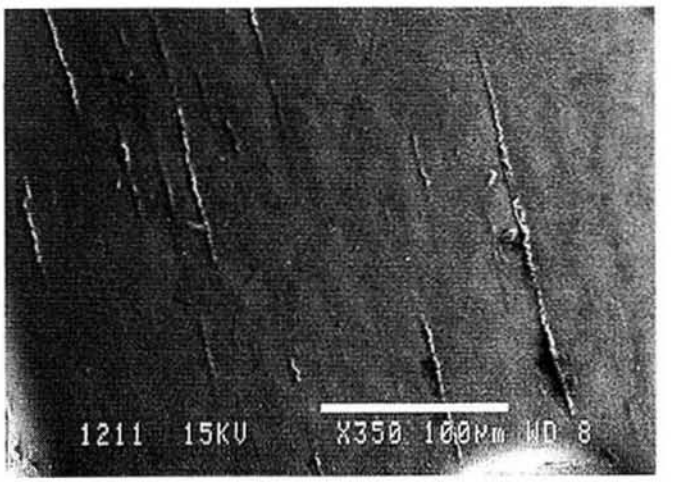

Figure 6. External faces of stent.

treated stents are reported in Figure 8. Elements distribution for EP and PA samples was similar while HT and AA samples exhibited very characteristic depth profiles. The AES depth profile of the NT stent is not shown because the stents were covered by a thicker oxide layer than the argon beam could sputter. Still, the NT stent oxide layer thickness was evaluated to be approximately 10 000 Å; its main composition was of Ti and O, and there was a random presence of Ni.

Oxide layer thicknesses of treated NiTi stents were derived from the O depth profile of samples. Table I summarizes the distribution of Ti, Ni, and O and oxide layer thicknesses obtained from depth profiles for each surface treated stent. AES depth profiles of treated samples indicated not only a variation in oxide thickness among different treatments, as reported in Table I, but also a significant difference between NT and treated stents. No significant difference in the oxide layer thickness could be observed before and after corrosion experiments for stents with the same surface treatment.

Before and after the corrosion experiments, XPS survey scans of the treated stents indicated the presence of Ti and O from the oxide layer and also other peaks such as Cu and C from the sample holder and the contamination. Again, a low concentration of other elements (<5%) was recorded and attributed to contamination during the preparation procedure and/or to the physiological solution. By considering the area of Ni and Ti peaks on the survey scans and their sensibility factors, the Ni/Ti ratio for each stent could be evaluated, as shown in Figure 9.

High resolution spectra of C, Ti, O, and Ni were performed to determine the nature of the bonding between elements. Our results show that all samples exhibited the same oxide chemical composition before and after the corrosion experiments. The presence of carbon on all samples (C—C, C—O, and C=O) was imputed to the contamina-

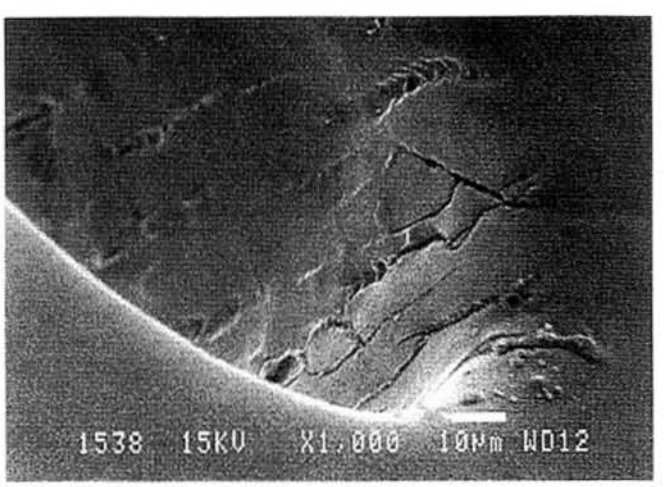

Figure 5. Presence of cracks on lateral face of devices at end point of 2 NiTi stent strut.

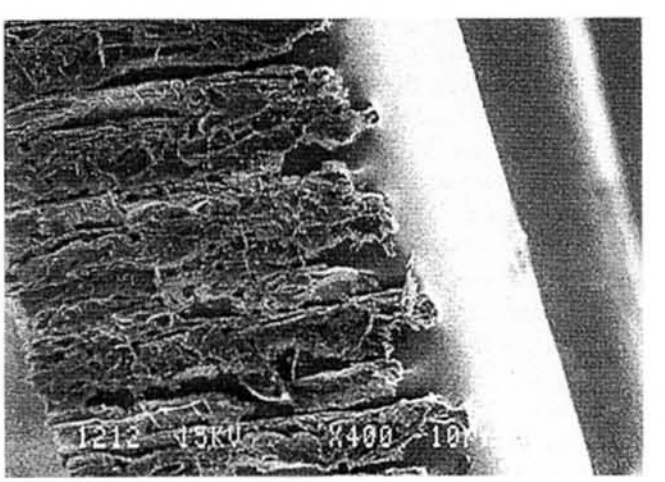

Figure 7. Lateral face of stent.

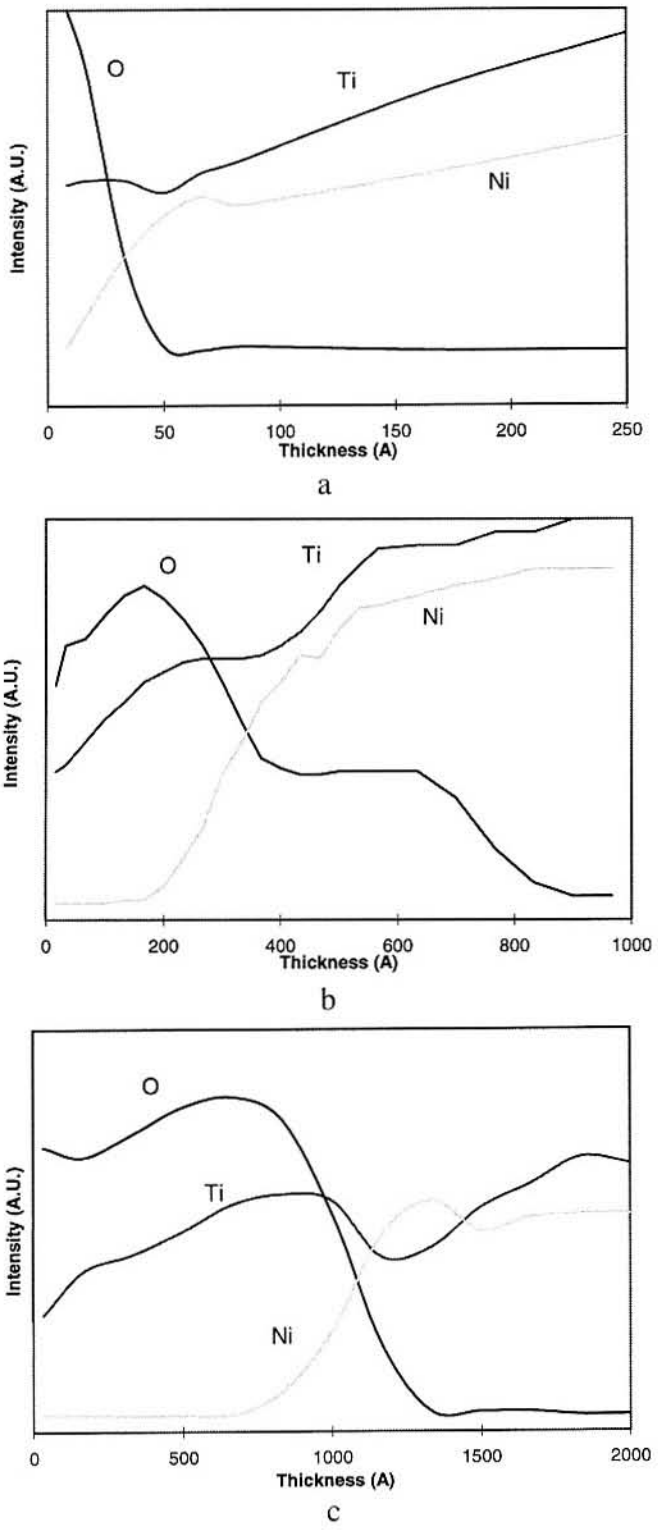

Figure 8. Typical AES depth profiles of surface treated NiTi stents for the distribution of oxygen (O)z, titanium (Ti) and nickel (Ni). (a) EP and PA, (b) AA, (c) HT.

tion of the stent and the sample holder by organic substances. The Ti spectrum for EP and PA stents was dominated by three peaks at 454.1, 456.4, and 458.8 eV, which

TABLE I. Description of Element Distribution and Oxide Layer Thickness

Surface Treatment	Ni, Ti, O Distribution	Oxide Layer Thickness (Å) Mean ± SD
EP	Ti, O, Ni[a] → Ni, Ti	34 ± 14
PA	Ti, O, Ni[a] → Ni, Ti	30 ± 1
AA	Ti, O → Ti, O, Ni → Ni, Ti	240 ± 78[b] 263 ± 143
HT	Ti, O, Ni[a] → Ni[c], Ti → Ni, Ti	911 ± 270

[a] Random Ni signal.
[b] Thickness of each oxide layer.
[c] Ni-rich region.

were assigned to metallic Ti (Ti^0), Ti_2O_3 (Ti^{+3}), and TiO_2 (Ti^{+4}), respectively.[16,17] HT and AA stents exhibited only one peak at 458.6 or 458.8 eV that was attributed to the TiO_2 form (Ti^{+4}). The O 1*s* high resolution spectrum consisted of TiO_2 (529.9 eV) from the oxide layer and C=O and C—O bondings due to contamination. The very low signal from the Ni 2*p* region rendered difficult the precise analysis of the chemical bonding for this element. However, the higher signal from the Ni 2*p* region on HT stents after corrosion made it possible to determine the position of two peaks at 854.7 and 856.4 eV that were assigned to NiO and Ni_2O_3, respectively.

DISCUSSION

In the literature, the corrosion behavior of NiTi alloys in physiological environments is not clearly established and is rather controversial. Sarkar et al. demonstrated that NiTi alloy was subject to an earlier breakdown of its passive film when compared to other implant materials (titanium,

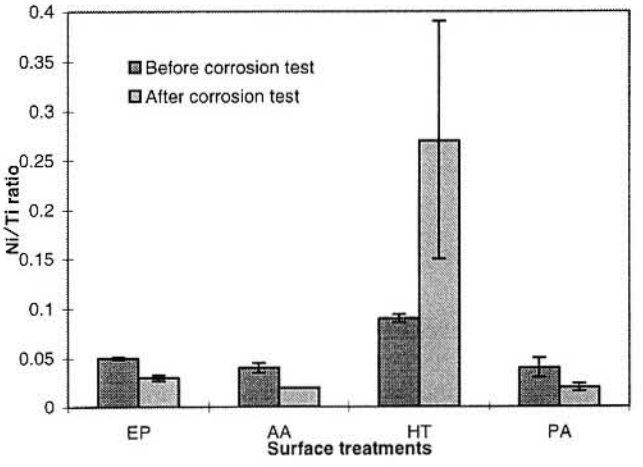

Figure 9. Ni/Ti ratio as a function of surface treatment before and after corrosion experiment.

stainless steel, and cobalt-chrome alloys) during potentiodynamic cyclic polarization tests.[18] On the other hand, Speck and Fraker showed that NiTi had a better resistance to corrosion, exhibiting a pitting potential during anodic polarization measurements more than 700 mV higher than 316L stainless steel, CoCrMo alloys, or CoNiMo alloys.[19] Finally, a study performed by Rondelli on the corrosion performance of several commercial implant-based materials showed that NiTi presents an intermediate pitting potential (~800 mV vs. SCE) inferior to Ti-6Al-4V (>1000 mV vs. SCE) but superior to AISI 316L (~400 mV vs. SCE) during potentiodynamic tests.[20] However, its corrosion resistance was significantly inferior to that of these two metals when potentiostatic scratch tests were performed. These results illustrate the variable corrosion behavior of the alloy given different test methodologies and possibly different surface conditions. The complex and slow process of repassivation of the NiTi alloy once the passive film has been damaged may also account for the different results discussed in the literature.[18] Furthermore, some studies showed that Ni could be selectively dissolved during the corrosion of NiTi.[21,22] The issue of nickel release in the physiological environment from an alloy is important because this element is frequently involved in hypersensitivity and toxic reactions.[23,24] Still, Xiao–Xiang et al. demonstrated that Ni release from NiTi can be significantly decreased by an appropriate oxidation treatment.[25] These findings emphasize the importance of controlling the nature and homogeneity of the NiTi oxide film by different surface treatments. Furthermore, results from our study emphasize the importance of surface conditions on the corrosion behavior of NiTi alloy.

Polarization curves (Fig. 1) demonstrated that all surface treatments improved the corrosion resistance of the NiTi stents in comparison with the NT stents. As shown in Figure 2, all treated stents presented an increase in pitting potential values, denoting a higher resistance to localized corrosion of treated samples. Furthermore, this improvement was more prominent in the EP and PA samples.

As observed by SEM, comparison of micrographs of treated and NT stents (Figs. 3, 4) before corrosion indicates an improvement in the topography after treatments that all produce a smoother surface. This uniformity of the oxide layer was accentuated for our EP and PA samples. Earlier studies on Ti showed that the morphology of the surface oxides strongly depends on the nature and microstructure of the underlying metal.[26,27] Our NT machined sample surfaces consisted of a plastically deformed layer. EP removed this layer, resulting in surfaces with a more homogeneous and uniform morphology. The oxide growth from this new underlying metal presented a new morphology with new characteristics. Subsequently, the improvement in corrosion resistance of our samples was explained either by improvement of surface uniformity or by growth of a less deformed oxide layer on the surface.

Microscopic analysis of stents after corrosion showed a difference in the corrosion behavior on different faces of the devices. Indeed, the lateral faces of the stents corroded faster than the external faces (Figs. 6, 7). This vulnerability of the lateral faces may be attributed to several factors: heterogeneity of the surface treatment or the presence of cracks in the amorphous surface layer. These were observed before the corrosion experiments (Fig. 5) and could have been caused by either the laser cutting process of the tubing or the stress concentration on these parts of the device during expansion. Also, as shown in Figure 6, machining marks rendered the external surface of the stents more vulnerable to corrosion on all samples. The importance of surface coating homogeneity for the corrosion resistance of NiTi alloy has been underlined by many authors.[8,9,17] The effect of stress and strain is not well established, but some studies have shown that these factors may play a role in the corrosion behavior of NiTi alloys.[28,29] Our SEM results demonstrated that a uniform and smooth oxide layer was a predominant factor for the improvement of the corrosion behavior of surface treated NiTi stents. The nonuniformity of the oxide layer on areas of high mechanical stress may therefore highlight the importance of strain on corrosion behavior.

Further, Auger analyses of the oxygen distribution demonstrated the effect of oxide thickness on the corrosion behavior. A variation of oxide layer thickness ranging from 10 000 Å (NT stents) to 30 Å (PA stents) was measured. When these results were related to those obtained for the corrosion behavior of the samples, it was possible to conclude that oxide layer thickness controlled less corrosion resistance than surface uniformity. Stents that resisted during corrosion were characterized by a thinner oxide layer (EP and PA stents) compared with the other treated and NT devices. Similar results (on plates heated at 900 °C) were obtained by Sohmura on the reliability of a thin oxide layer for improvement of corrosion resistance of NiTi.[10]

Because of the stent geometry, the lateral and external faces are oriented differently with respect to the argon sputter beam and analyzer. This situation makes it difficult to compare the composition and oxide layer thickness of these two faces. Thus, we were unable to discern to what extent the thickness and composition of the oxide layer controlled the corrosion behavior of these parts of the stents.

Ni/Ti ratios determined by XPS survey scans (Fig. 9) demonstrated a higher value associated with HT stents than with the other surface treated devices. Moreover, while AA, EP, and PA samples were characterized by a decrease in this ratio after the corrosion experiments, the HT Ni/Ti ratio significantly increased. The higher ratio measured for HT stents may be attributed to the diffusion of more Ni elements on the alloy surface. Diffusion of Ni in a defective Ti oxide layer has already been shown in many studies.[11,30–32] These findings suggest that the oxide layer on HT stents may have been defective (nonstochiometric) and promoted the diffusion of Ni; however, confirmation of this hypothe-

sis was not obtained during this work. Transmission electron spectroscopy or more extensive XPS studies should be undertaken to confirm this assumption.

XPS results on the similar chemical composition of the surface oxide layer for EP and PA stents were in accordance with our Auger analyses. Even though AES depth profiles showed that the surface oxide of HT devices seemed to be composed of only Ti and O, Ni signals recorded during XPS scans may be due to the Ni-rich region observed on these stents above the NiTi bulk material. Also, the random nature of Ni in the oxide may explain that the Ni signal was not recorded on those stents during our Auger analyses. Chan et al. attributed this Ni signal in the oxide layer to segregation of Ni that can occur in NiTi alloys under certain oxidation conditions.[17]

XPS high resolution spectra also showed that our surface treatments encouraged the growth of a Ti oxide layer to the detriment of Ni oxidation. This finding is very favorable for good biocompatibility of surface treated NiTi stents, because the Ti oxide layer has been shown to be very stable and protective of Ti implant materials and is responsible for its high tissue compatibility.[26] This preferential oxidation process of NiTi alloy has already been described by other authors. A study of the oxidation process of NiTi demonstrated that formation of TiO_2 was predominant and oxidation of Ni was insignificant.[33] From a thermodynamic standpoint, formation of a TiO_2 oxide layer on NiTi is a more favorable process than oxidation of Ni, which explains the very low concentration of Ni in our samples.[17] On EP and PA samples it is evident that this Ti oxide coating is thin, because peaks from the underlying substrate (metallic Ti) were apparent in the high resolution spectra of this element.

From our Auger depth profile analyses and XPS results, it seems that except for the nitric acid PA samples, surface treatment of NiTi stents affects both the composition and thickness of the oxide layer of the devices. However, no direct relation could be established with respect to the effect of the composition of the oxide layer on the corrosion resistance, because of the variation of the layer as a function of its thickness and uniformity.

CONCLUSION

Results showed that EP, HT, AA, and nitric acid PA of NiTi improved the corrosion behavior of the alloy. Surface topography analyses by SEM and chemical analyses by AES and XPS provided relations between surface physicochemical properties and corrosion behavior. Our study demonstrated that the surface treatments performed on NiTi stents modified the topography, thickness, and composition of the oxide layer. These parameters influenced the corrosion behavior of our treated samples to different extents.

SEM micrographs indicated that the surface condition plays an important role in NiTi stent corrosion resistance. Treated samples with smooth and uniform surfaces demonstrated a higher corrosion resistance than NT ones that possessed a very porous and irregular oxide layer. From the AES results it seems that corrosion resistance of NiTi stents is not directly related to oxide layer thickness. Indeed, the best corrosion behavior was observed for stents with the thinnest and most uniform oxide layers (EP and PA). Our XPS and Auger analyses revealed the effect of surface treatments on promoting the growth of a more protective Ti oxide layer on the surface of the alloy and emphasized the different oxide compositions of the scale. In conclusion, our results show that oxide layer uniformity is a predominant factor for the protection of NiTi stents against corrosion.

The present study has important implications for the final steps of fabrication of NiTi implants. Our results show that EP NiTi significantly increases the corrosion resistance of the alloy. Subsequent treatments such as AA, HT, and PA in a nitric acid solution seem to have a detrimental or slightly beneficial effect. Moreover, these additional steps may increase the cost of stent production.

The authors gratefully acknowledge the financial and material support of NSERC (Canada) and Nitinol Devices & Components Inc. (California). They also want to thank S. Poulin from ESCALAB and S. Martel from $(CM)^2$ (École Polytechnique of Montreal, Canada) for their technical help and advice.

REFERENCES

1. Sigwart, U.; Puel, J.; Mirkovitch, V.; Joffre, F.; Kappenberger, L. Intravascular stents to prevent occlusion and restenosis after transluminal angioplasty. N. Engl. J. Med. 316(12):701–706; 1987.
2. Serruys, P. W.; et al. A comparison of balloon-expandable-stent implantation with balloon angioplasty in patients with coronary artery disease. N. Engl. J. Med. 331:489–495; 1994.
3. Fishman, D. L.; et al. A randomized comparison of coronary-stent placement and balloon angioplasty in the treatment of coronary artery disease. N. Engl. J. Med. 331:496–501; 1994.
4. Lau, K. W.; Sigwart, U. Intracoronary stents. Ind. Heart J. 43(3):127–139; 1991.
5. Berger–Gorbet, M.; Broxup, B.; Rivard, C. H.; Yahia, L'H. Biocompatibility testing of NiTi screws using immunohistochemistry on sections containing metallic implants. J. Biomed. Mater. Res. 32:243–248; 1996.
6. Assad, M.; Yahia, L'H.; Desrosiers, E. A.; Lombardi, S.; Rivard, C. H. Cyto-compatibility testing of Ni-Ti. Edited by Pelton, A.; Hodgson, D.; Duerig, T., Eds. Shape Memory and Superelastic Technologies Conference Proceedings, Pacific Grove, CA; 1994:215–220.
7. Shabalovskaya, S. A.; Cunnick, J.; Anderegg, J.; Harmon, B.; Sachdeva, R. Preliminary data on *in vitro* study of proliferative rat spleen cell response to Ni-Ti surface characterized using ESCA analysis. Pelton, A.; Hodgson, D.; Duerig, T., Eds. Shape Memory and Superelastic Technologies Conference Proceedings, Pacific Grove, CA: 1994:209–214.
8. Putters, J. L. M.; Kaulesar Sukul, D. M. K. S.; de Zeeuw, G. R.; Bijma, A.; Besselink, P. A. Comparative cell culture effects of shape memory metal (Nitinol®), nickel and titanium: a biocompatibility estimation. Eur. Surg. Res. 24:378–382; 1992.

9. Villermaux, F.; Tabrizian, M.; Yahia, L'H.; Meunier, M.; Piron, D. L. Excimer laser treatment of NiTi shape memory alloy biomaterials. Appl. Surface Sci. 110:62–66; 1997.
10. Sohmura, T. Improvement in corrosion resistance in Ti-Ni shape memory alloy for implant by oxide film coating. World Biomaterial Congress Proceedings, Kyoto, Japan; 1988:574.
11. Espinos, J. P.; Fernandez, A.; Gonzalez–Elipe, A. R. Oxidation and diffusion processes in nickel-titanium oxide systems. Surface Sci. 295:402–410; 1993.
12. Bloyce, A.; Morton, P. H.; Bell, T. Surface engineering of titanium and titanium alloys. ASM Handbook, Vol. 5. Metals Park, OH: ASM International; 1994:835–851.
13. Wisbey, A.; Peter, P. J.; Tuke, M. Effect of surface treatment on the dissolution of titanium-based implant materials. Biomaterials 12:470–473; 1990.
14. Annual Book of ASTM Standards, Vol. 13.01. Philadelphia, PA: ASTM; 1996:Section 13.
15. Lumsden, J. B. X-ray photoelectron spectroscopy. Metals Handbook, Vol. 10, 9th edition, Philadelphia, PA: ASTM; 1986:568–580.
16. Moulder, J. F.; Stickle, W. F.; Sobol, P. E.; Bomben, K. D.; Chastain, J., Ed. Handbook of X-Ray Photoelectron Spectroscopy. New York: Perkin–Elmer Corporation; 1992.
17. Chan, C.-M.; Trigwell, S.; Duerig, T. Oxidation of a NiTi alloy. Surface Interference Anal. 15:349–354; 1990.
18. Sarkar, K.; Redmond, W.; Schwaninger, B.; Goldberg, A. J. The chloride corrosion behavior of four orthodontic wires. J. Oral Rehabil. 10:121–128; 1983.
19. Speck, M.; Fraker, A. C. Anodic polarization behavior of Ti-Ni and Ti-6Al-4V in simulated physiological solutions. J. Dent. Res. 59:1590–1595; 1980.
20. Rondelli, G. Corrosion resistance tests on NiTi shape memory alloy. Biomaterials 17:2003–2008; 1996.
21. Okuyama, M.; Yahia, L'H.; Piron, D. L.; Lombardi, S. Biocompatibility of nickel-titanium shape memory alloy: an *in vitro* electrochemical study. Biomater. Living Syst. Int. 3:145–160; 1995.
22. Oshida, Y.; Sachdeva, R. C. L.; Miyazaki, S. Microanalytical characterization and surface modification of TiNi orthodontic archwires. Bio-Med. Mater. Eng. 2:51–69; 1992.
23. Williams, D. F. Toxicology of implanted metals. Williams, D. F., Ed. Fundamentals Aspects of Biocompatibility, Vol. II. Boca Raton, FL: CRC Press; 1981:45–61.
24. Takamura, K.; Hayashi, K.; Ishinishi, N.; Yamada, T.; Sugioka, Y. Evaluation of carcinogenicity and chronic toxicity associated with orthopedic implants in mice. J. Biomed. Mater. Res. 28:583–589; 1994.
25. Xiao–Xiang, W.; Zhi–Yuan, M.; Zhen–Wang, C. The oxide film and its effect on shape memory effect and biocompatibility in TiNi alloy. Chu, Y.; Tu, H., Ed. Shape Memory Materials '94. International Academic Publishers; 1994:621–625.
26. Lausmaa, J.; Mattsson, L.; Rolander, U.; Kasemo, B. Chemical composition and morphology of titanium surface oxides. Mater. Res. Soc. Symp. Proc. 55:351–359; 1986.
27. Larsson, C.; Thomsen, P.; Lausmaa, J.; Rodhal, M.; Kasemo, B.; Ericson, L. E. Bone response to surface modified titanium implants: studies on electropolished implants with different oxide thicknesses and morphology. Biomaterials 15:1062–1074; 1994.
28. Villermaux, F.; Tabrizian, M.; Yahia, L'H.; Czeremuskin, G.; Piron, D. L. Corrosion resistance improvement of NiTi osteosynthesis staples by plasma polymerized tetrafluoroethylene coating. Bio-Med. Mater. Eng. 6:241–254; 1996.
29. Montero–Ocampo, C.; Lopez, H.; Salinas Rodriguez, A. Effect of compressive straining on corrosion resistance of a shape memory Ni-Ti alloy in Ringer's solution. J. Biomed. Mater. Res. 32:583–591; 1996.
30. Bourgeois, S.; Diakité, D.; Jomard, F.; Perdereau, M.; Poirault, R. Nickel deposition on $TiO_2(100)$: Characterization by AES and SIMS. Surface Sci. 217:78–84; 1989.
31. Gonzalez–Elipe, A. R.; Fernandez, A.; Espinos, J. P.; Munuera, G. Role of hydrogen in the mobility of phases in Ni-TiO_x systems. J. Catal. 131:51–59; 1991.
32. Munuera, G.; Gonzalez–Elipe, A. R.; Espinos, J. P. XPS study of phase mobility in Ni/TiO_2 systems. Surface Sci. 211/212:1113–1122; 1989.
33. Chuprina, V. G. A study of the process of oxidation of titanium nickelide II. Phase composition of the scale. Sov. Powder Metal. Metal Ceram. 28:468–472; 1989.